High-Temperature Corrosion And Materials Applications
George Y. Lai, editor, p335-358
DOI: 10.1361/hcma2007p335

CHAPTER 12

Waste-to-Energy Boilers and Waste Incinerators

12.1 Introduction

Municipal solid waste (MSW) is a combination of residential, commercial, and industrial refuse. Historically, the typical means of disposal of this refuse has been landfilling. A novel approach in recovering the energy from this "resource" in boilers for electricity generation and minimizing the landfill requirements began in the 1960s in Europe. It became apparent from these early European boilers that corrosion of the boiler tube materials was a major obstacle for operating these so-called waste-to-energy (WTE) boilers (Ref 1, 2). Managing the corrosion problems continues to be a big challenge for operators of modern boilers worldwide. This chapter focuses on the corrosion issues related to boilers burning municipal solid waste.

12.2 Fuels, Combustion Environments, and Boilers

Municipal solid waste typically contains paper and paperboard, plastics, rubber, textile, leather, batteries, food waste, yard waste, metal, glass, and other miscellaneous materials. This type of fuel is very heterogeneous and varies greatly by geographic location, country, and "culture." In North America, typical constituents of the MSW in 1990 were paper and paperboard (34.2–40.0%), plastics (7.2–9.2%), food waste (7.3–8.5%), yard waste (17.6–19.9%), metal (8.1–9.6%), glass (7.7–9.7%), and other (10.3–13.2%) (Ref 3). Polyvinyl chloride (PVC) plastic is a dominant source of chlorine, which is a major corrosive constituent making the combustion environment corrosive to boiler tube materials. Polyvinyl chloride contains about 36 wt% chlorine (Ref 4). Rubbers such as Hypalon, chloroprene, and neoprene also contain high concentrations of chlorine (Ref 4). Other waste constituents that can contribute to corrosive environments under combustion are batteries (automobile batteries, button-type batteries in watches and calculators, alkaline, zinc, nickel, and cadmium batteries) and consumer electronics. Batteries contribute lead and cadmium; household batteries contribute cadmium; and consumer electronics contribute both lead and cadmium (Ref 5). Rademakers et al. (Ref 6) reported their calculation of the heavy metal composition of Dutch solid waste based on 1994 data in g/kg waste: 0.01 Cd, 0.0004 to 0.0006 Hg, 0.22 to 0.56 Pb, 0.02 to 0.04 Sb, 0.63 to 1.04 Zn, 0.01 As, 3.96 to 6.89 Cl, 0.11 to 0.19 Br, 0.1 to 0.2 F, and 1.48 to 2.96 S. During combustion, these heavy metals can react with chlorine to form some low-melting-point chlorides, thus causing severe boiler tube material corrosion problems. Corrosion mechanisms are discussed in the next section.

There are primarily two types of combustion technologies, namely, mass-burning and refuse-derived fuel (RDF) burning. For mass-burning units, the fuel, which is not segregated except for appliances, furniture, and other large articles, burns in the as-received condition. In RDF units, on the other hand, the fuel is segregated, classified, and shredded to size. Metals and glass are typically removed from RDF fuel prior to combustion. Thus, RDF fuel has a higher heating value than that of a mass-burning unit. A small number of boilers in use today are based on the fluidized-bed technology. The mass-burning unit uses a mechanical stoker to feed the fuel onto a grate where the fuel is combusted. For most RDF units, the fuel is blown into the furnace sidewalls through an RDF burner with a fuel-distribution impeller (Ref 3). Most RDF units burn the fuel in

suspension (Ref 3). RDF units also employ moving grates.

Combustion gas temperatures are generally at or below approximately 1090 °C (2000 °F) in mass-burning units and approximately 1315 to 1370 °C (2400 to 2500 °F) in RDF units (Ref 7). The guidelines for solid waste combustion introduced by the European authorities require that the temperature should be above 850 °C (1560 °F) for a 2 s residence time at the level 1 m above the secondary or tertiary air (Ref 6). The MSW boilers operate at much lower steam pressures and temperatures compared with coal-fired utility boilers, as discussed in Chapter 10. Kubin (Ref 7) reported that Ogden Martin boilers in the United States typically operated at steam pressures of 4 to 6 MPa (615 to 880 psig) and temperatures of 370 to 440 °C (700 to 830 °F) for mass-burning units, and steam pressures of 4.5 to 6 MPa (665 to 900 psig) and temperatures of 370 to 440 °C (700 to 830 °F) for RDF units.

These pressures and temperatures appear to be representative of other WTE boilers in the United States. For example, two boilers at the Wheelabrator Concord facility operate at a steam pressure of 650 psig (4.5 MPa) and a temperature of 400 °C (750 °F), and two at the Wheelabrator Spokane facility operate at 6.2 MPa (900 psig) and 440 °C (830 °F) steam (Ref 8), with some other Wheelabrator boilers operating at higher pressures and temperatures (Ref 9). Some of the European boilers operate at higher steam pressures and temperatures. For example, the boilers at Ivry Paris (France) operate at 7.5 MPa (1103 psig, or 75 bar) and 480 °C (900 °F) steam, at HKW Mannheim (Germany) at 8 MPa (1176 psig, or 80 bar) and 500 °C (930 °F) steam, at BSR Berlin (Germany) at 7.5 MPa (1088 psig, or 74 bar) and 420 °C (790 °F) steam, and at EVO Oberhausen (Germany) at 7 MPa (1029 psig, or 70 bar) and 480 °C (896 °F) steam (Ref 10). Early European WTE boilers developed in the 1960s were designed to operate at higher steam pressures and temperatures, particularly those in Germany, with one in Mannheim operating at 12.5 MPa/530 °C (1800 psig/980 °F) steam and another one in Munich at 18 MPa/540 °C (2650 psig/1000 °F) steam (Ref 1). Higher steam temperatures result in higher tube metal temperatures and thus more serious corrosion problems.

Combustion of the MSW fuel is significantly different from that of coal or oil because the solid waste is a heterogeneous fuel. In addition, the fuel contains numerous impurities that include chlorine, sulfur, sodium, potassium, cadmium, zinc, lead, and other heavy metals. Because of these impurities, combustion of this fuel generates a very corrosive environment that causes serious corrosion problems for boiler tube materials. Gaseous combustion products include N_2, O_2, CO_2, H_2O, SO_2, HCl, HF, and other gaseous impurities such as CO and HBr. These gaseous constituents are often measured by plant operators. Examples of these flue gas compositions measured in mass-burning units at different plants are shown in Table 12.1 (Ref 7, 11–13). However, vapors of metal chlorides and sulfates are also produced during combustion. These compounds are normally not quantified by plant personnel. Many of these metal chlorides exhibit high vapor pressures and/or low melting points. Some physical properties of many metal chlorides can be found in Chapter 6 "Corrosion by Halogen and Halides." As is discussed in this chapter, some of these metal chlorides are primarily responsible for the corrosion of the boiler tube materials.

The furnace is typically enclosed by four walls (rear, front, and two side walls) using a tube-membrane construction (i.e., individual tubes are connected by narrow plates). These tube-membrane walls, which are commonly referred to as "waterwalls," provide heat-absorbing

Table 12.1 Examples of flue gas compositions generated by different WTE mass-burning boilers

	Composition, vol%			
Gas	Ogden-Martin (US)(a)	Saint Ouen (France)(b)	Richtlinien (Germany)(c)	Kuririn (Japan)(d)
O_2	8.5–9.5	9–10	NR	9.1
CO_2	8–9	9–12	NR	11.1
SO_2	100–200 ppm	90–130 ppm	100–2000 ppm	40 ppm
HCl	400–600 ppm	600–1200 ppm	560–2240 ppm	810 ppm
HF	5–20 ppm	20–40 ppm	…	…
CO	…	<20 ppm	64–640 ppm	42 ppm
H_2O	13–15	NR	NR	21.4
N_2	bal	bal	NR	bal

NR, not reported. (a) Source: Ref 7. (b) Source: Ref 11. (c) Source: Ref 12. (d) Source: Ref 13

surfaces for converting the water inside the tubes to steam as the water rises from the bottom of the waterwall. At the top of the waterwall tubes, a mixture of steam and water leaves the waterwall tubes and enters the steam drum where steam is separated from water. The furnace waterwall typically operates with water at a saturation temperature. Thus, the temperature of the water/steam in the waterwall tubes, which depends on the pressure of the water/steam, is generally at or below 277 °C (530 °F) (Ref 14). The ranges of the waterwall tube metal temperatures were cited to be 260 to 293 °C (500 to 560 °F) (Ref 7), 260 to 290 °C (500 to 550 °F) (Ref 15), and 260 to 315 °C (500 to 600 °F) (Ref 16). For higher-pressure boilers, the temperature of the steam will be higher. The steam from the steam drum after separating from water is then further heated in superheaters (typically two superheaters—primary and secondary or final superheaters) to higher temperature in the convection path before it is delivered to turbines for electricity generation. The combustion flue gas exits from the furnace at the top and then enters into the convection path, flowing typically through the superheater, then the boiler bank, and the economizer. The flue gas temperature entering into the superheater may vary from approximately 650 to 900 °C (1200 to 1650 °F).

Figure 12.1 shows a schematic of a mass-burning unit. For some mass-burning units, screen tubes are installed in front of the superheater to lower the temperature of the flue gas entering into the superheater section. In some other mass-burning units, there are additional gas passes (one or more additional walls to allow flue gas to pass through in the convection path) to allow the flue gas stream to lower its temperature before entering into the superheater section. This type of design is shown schematically in Fig. 12.2 (Ref 17). Licata et al. (Ref 17) indicated that passing flue gas through two 180° turns and one 90° turn prior to entering the superheaters can not only lower the flue gas temperature but also remove particles from the flue gas stream. In addition, the flue gas stream can achieve better mixing to minimize local reducing conditions (Ref 17). Figure 12.3 shows a schematic of an RDF unit. Carbon steels and sometimes low-alloy steels are typical construction materials for waterwalls, screen tubes, the boiler bank, and economizer. For superheaters, carbon and low-alloy steels are typically the materials of construction.

This chapter focuses mainly on waterwalls and superheaters that have experienced severe corrosion problems. Also discussed are the latest protection methods against corrosion and

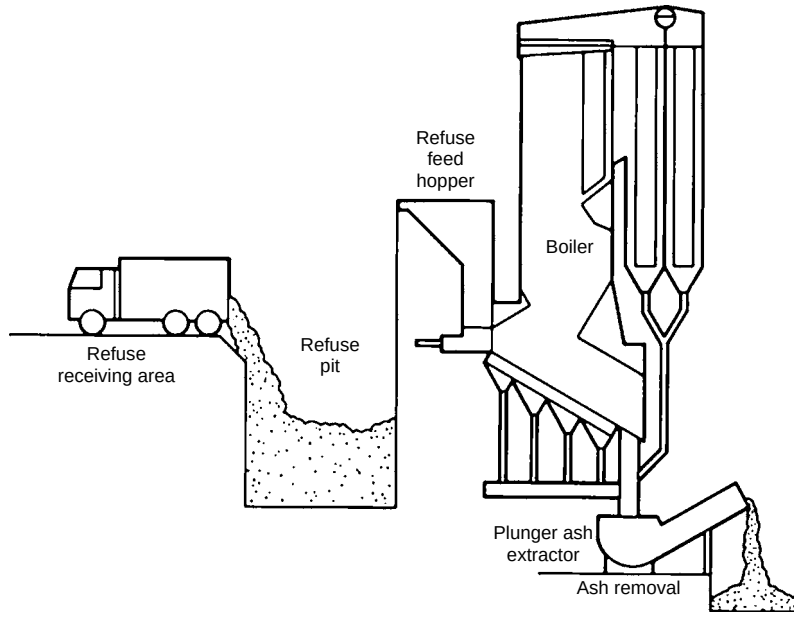

Fig. 12.1 Mass-burning unit, with a grate where the fuel burns and the superheater right above the arch (or bull nose) in the upper furnace, followed by a boiler bank and an economizer in the convection pass downstream of the superheater. Source: Ref 3

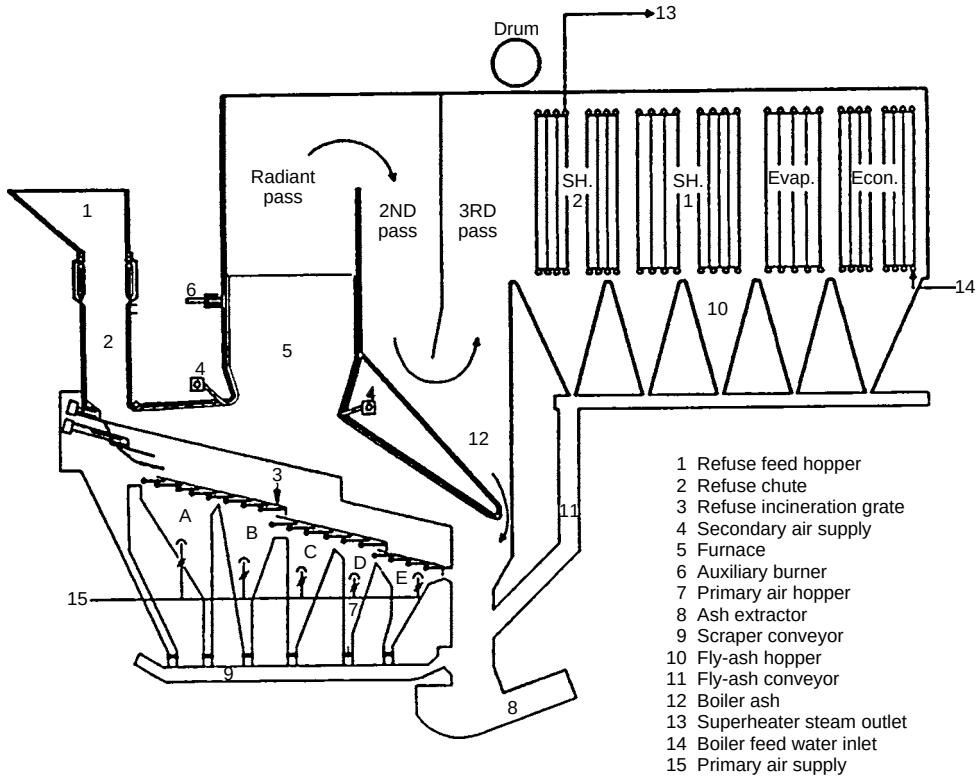

Fig. 12.2 Mass-burning unit of different design involving multiple passes for the flue gas stream before entering the superheaters. Also shown is the grate where the fuel is combusted. Source: Ref 17

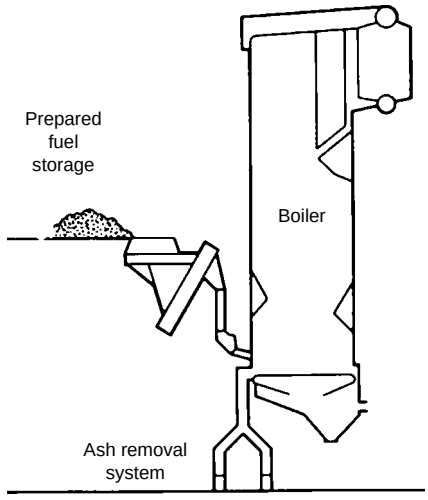

Fig. 12.3 Refuse-derived fuel unit, with superheaters (right above the nose arch or bull nose) and a boiler (generating) bank in the convection pass. The bottom of the furnace is a traveling grate. Source: Ref 3

erosion/corrosion at these two critical areas in the boiler.

12.3 Boiler Tube Fireside Corrosion Problems

Materials problems and high wastage rates experienced by furnace waterwalls and superheaters in numerous waste-to-energy plants worldwide have been extensively reviewed by Krause (Ref 1), Sorell (Ref 2), and Krause and Wright (Ref 18). Many of the early boilers, particularly European boilers, suffered severe boiler tube failure problems. A boiler (410 °C, or 770 °F, and 5 MPa, or 725 psig steam) at the Issy plant in Paris suffered tube failures in the side wall after only about 5000 h of operation, and the same boiler suffered serious superheater corrosion problems from the start of the operation (Ref 1). In a boiler (525 °C, or 980 °F, and 12 MPa, or 1800 psig steam) in Mannheim, Germany, the furnace wall tubes failed only after

3000 h of operation, and superheater tube failed after only 2000 h of operation (Ref 1). The first U.S. WTE boiler with relatively low steam temperature (320 °C, or 610 °F) in Nashville, TN, suffered both waterwall and superheater failure within the first year of operation (Ref 18). Many other tube failures have been cited in Ref 1, 2, 18–21). All these initial boiler tubes materials were carbon and low-alloy steels with no corrosion protection.

Modern WTE boilers have increasingly used various corrosion protection methods to protect waterwalls, superheaters, and boiler banks against corrosion and erosion/corrosion. Many boilers with no corrosion protection for their waterwalls and superheaters continue to suffer premature failures. Figure 12.4 shows an example of a tube failure at the waterwall in one boiler after only 8 months of operation (Ref 22). One effective corrosion protection method for the furnace waterwalls was developed in the 1985 to 1986 period by using alloy 625 overlay cladding, which was applied on-site in an RDF boiler in Lawrence, MA using an automatic gas metal arc welding (GMAW) process (Ref 23). A total of about 21,000 lb of alloy 625 weld overlay metal was applied to this boiler. The performance of the waterwall overlay of alloy 625 in this first overlaid waterwall proved to be very successful during the next 3 to 4 years of boiler operation. Between 1989 and 1990, a total of about 260,000 lb of alloy 625 weld overlay metal was applied to the waterwalls of 29 boilers (Ref 23). Alloy 625 overlay has been found to provide dramatic reduction in metal loss in areas where carbon or low-alloy steels have suffered unacceptable wastage rates (Ref 7, 16, 22–25). For mass-burning units, the waterwalls are typically protected by alloy 625 weld overlay above the refractory lining at the lower, high-radiant section of the boiler (Ref 9). The waterwalls in an RDF boiler are generally fully protected with alloy 625 weld overlay (Ref 9). Kubin (Ref 7) indicated that all RDF boiler waterwalls for Ogden plants were virtually fully covered with alloy 625 weld overlay.

In many plants, alloy 625 as an outer tube cladding for corrosion protection of superheaters (with higher metal temperatures) has also proved to provide significant reduction in tube-wall wastage rates compared to carbon and low-alloy steels (Ref 10, 22, 24). Excellent performance was observed for alloy 625 overlay superheater tubes in a boiler in Europe, as shown in Fig. 12.5. The cladding can either be in a form of weld overlay (Ref 24) or coextruded tube cladding (Ref 10). In some plants, however, alloy 625 cladding in superheaters was found to experience high wastage rates (Ref 10, 12, 22, 24). This is illustrated in Fig. 12.6 (Ref 10, 22). The wastage rates ranged from less than 10 mpy to hundreds of mpy. Superheater corrosion appears to be highly dependent on the individual boiler. Possible corrosion mechanisms involved in WTE environments are discussed in the next section.

Fig. 12.4 Carbon steel waterwall suffering blown tubes due to high wastage rates resulting in significant tube-wall thinning after 8 months of service in a WTE boiler. Courtesy of Welding Services Inc.

12.4 Corrosion Mechanisms

As described in Section 12.3, the furnace waterwalls and superheaters made of carbon or low-alloy steels suffered severe wastage problems in numerous boilers, experiencing tube failures after only thousands of hours of operation. Corrosion was the result of exposure to the combustion products generated during the combustion of MSW. Typical gaseous components generated during combustion are O_2, CO_2, H_2O, SO_2, and HCl with HF in some units. In some cases, local areas at the waterwall may be in reducing conditions. In those local furnace wall areas, there could be some CO present. Among these gaseous components, HCl is considered to be the most corrosive. In general, the level of HF, if present, is significantly lower than that of HCl (see Table 12.1). Thus, HF plays no significant role in corrosion of boiler tubes.

Carbon and low-alloy steels are very susceptible to corrosion by HCl at elevated temperatures. The level of HCl generated in combustion of MSW fuel is typically in the range of 100 to 2000 ppm. The tube metal temperatures of the waterwall, although depending on the operating pressure of the boiler along with other factors, are generally in the range of 260 to 315 °C (500 to 600 °F). The superheater tube metal temperatures are generally in the range of 370 to 540 °C (700 to 1000 °F), depending on the steam temperature, along with other factors. A brief review of the corrosion data in terms of the direct HCl corrosion is discussed below to see whether HCl

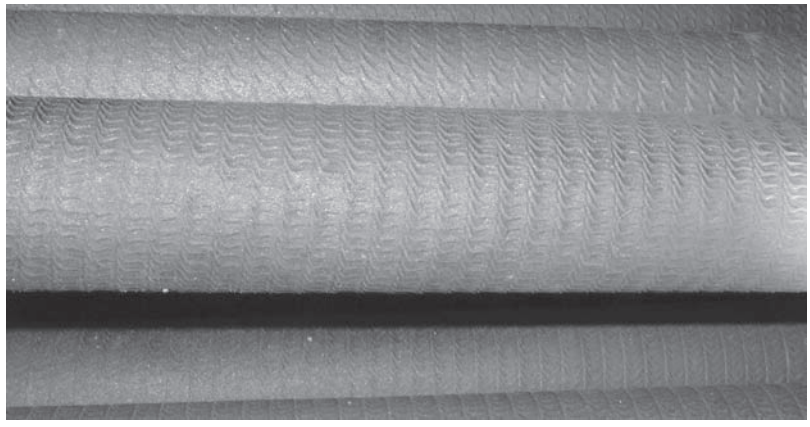

Fig. 12.5 Alloy 625 overlay superheater tubes (on 15Mo3 steel substrate) after 4.5 years of service in a superheater producing 405 °C (760 °F)/42 bar (609 psi) superheated steam, showing no evidence of corrosion or erosion/corrosion. Source: Ref 24

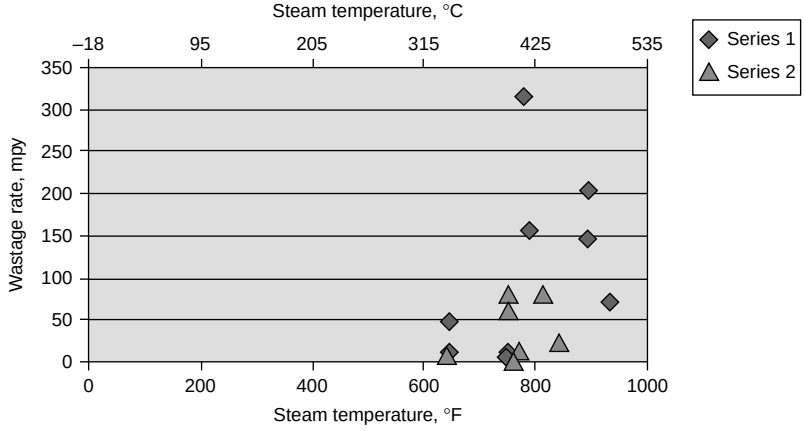

Fig. 12.6 Wastage rates as a function of steam temperature for alloy 625 cladding in weld overlay tubes and coextruded tubes tested as part of superheater tube bundles at various WTE boilers. Source: Ref 10, 22

Table 12.2 Corrosion rates in terms of metal loss for iron- and nickel-base alloys at indicated temperatures for 1008 h in N_2-10O_2-50ppmSO_2-500ppm HCl

	Metal loss					
	at 425 °C (800 °F)		at 480 °C (900 °F)		at 590 °C (1100 °F)	
Alloy	µm/yr	mpy	µm/yr	mpy	µm/yr	mpy
Type 316	0.07	0.003	2.54	0.1	5.08	0.2
Type 347	0.09	0.004	2.29	0.09	7.11	0.28
Alloy 800HT	0.07	0.003	1.02	0.04	5.33	0.21
Alloy 825	0.02	0.0008	1.27	0.05	2.54	0.1
Alloy 600	0.04	0.002	2.03	0.08	3.05	0.12
Alloy 625	0.02	0.0008	1.78	0.07	2.79	0.11

1.0 µm = 0.001 mm = 0.0394 mil. Source: Ref 27

corrosion can be responsible for severe waterwall and superheater corrosion.

Paul and Daniel (Ref 26) conducted laboratory tests at 315 °C (600 °F) for 720 h in simulated flue gas environments with one being an oxidizing atmosphere (N_2-2.6O_2-15.0CO_2-11.9H_2O-1000ppmSO_2-1000ppmHCl) and the other a reducing atmosphere (N_2-11.4CO_2-7.0CO-4.4H_2-11.9H_2O-1000ppmHCl). Specimens were not coated with salts nor covered with ash deposits. Both environments, containing about 1000 ppm HCl, showed that the corrosion rates for both carbon steel (SA178C) and Type 304 were less than 0.25 mm/yr (<10 mpy). Smith and Ganesan (Ref 27) conducted extensive tests in simulated flue gas environments with HCl concentrations varying from 500 ppm to 10% and temperatures from 425 °C (800 °F) to 590 °C (1100 °F). Corrosion rates were found to be quite low for austenitic stainless steels and nickel-base alloys at temperatures up to 590 °C (1100 °F) in flue gas environment containing 500 ppm HCl (Table 12.2). Even for the environment containing 4% HCl, the nickel-base alloys (alloys 825, 600, and 625) continued to show low corrosion rates. However, austenitic stainless steels exhibited high corrosion rates. This is illustrated in Table 12.3. A level of 4% HCl was more than an order of magnitude higher than what can be expected in a refuse-fired combustion environment, and the temperature of 590 °C (1100 °F) was much higher than the superheater metal temperature of current WTE boilers. Nevertheless, alloy 625 as either coextruded cladding or weld overlay was observed to suffer wastage rates of more than 1.3 mm/yr (>50 mpy) in some aggressive refuse-fired boilers (see Fig. 12.6). Table 12.3 shows that alloys 625 suffered a corrosion rate of about 1.53 mm/yr (60.4 mpy) when HCl was increased to 10% in the environment. Additional data for nickel-base alloys are shown in Table 12.4 (Ref 27). Devisme et al. (Ref 28) conducted tests in Ar-5HCl and Ar-5HCl-10O_2 environments at 600 °C (1110 °F), showing much higher corrosion rates in an oxidizing environment. However, the test tempered was much higher than the current superheater metal temperature. Their test results are summarized in Table 12.5. More corrosion data in halogen and halide environments are available in Chapter 6.

Table 12.3 Corrosion rates in terms of metal loss for iron- and nickel-base alloys at 590 °C (1100 °F) for 72 h in N_2-9O_2-12CO_2-100ppmSO_2-4 and 10HCl

	Metal loss			
	4% HCl		10% HCl	
Alloy	µm/yr	mpy	µm/yr	mpy
Type 316	914.4	35.7	…	…
Type 347	1244.6	48.5	…	…
Alloy 800HT	73.66	2.9	…	…
Alloy 825	20.32	0.8	1066	42.0
Alloy 600	25.4	1.0	1219	47.5
Alloy 625	15.75	0.6	1549	60.4

1.0 µm = 0.001 mm = 0.0394 mil. Source: Ref 27

It is generally agreed that chlorine in the fuel is an important cause of corrosion problems of boiler tubes. However, from the previous discussion, the direct corrosion of HCl, a gaseous component that formed when the chlorine in the fuel is combusted in the boiler, is not likely to be primarily responsible for the boiler tube corrosion. In Section 12.2, it was explained that there are a number of heavy metals, such as lead (Pb), zinc (Zn), cadmium (Cd), arsenic (As), and tin (Sb), along with alkali metals (i.e., Na, K) that are present in MSW. These metallic elements can react with chlorine to form various chlorides that have very low melting points. Many investigators (Ref 12, 14, 16, 20, 24, 29, 30) have considered that corrosion attack by low melting point chlorides is a principal mode of corrosion for boiler tubes in WTE plants.

Kawahara and Kira (Ref 31) observed that the corrosion rate of carbon steel changed to a much higher rate above approximately 300 °C (150 °F), which corresponded to the melting point of the deposits collected from the tube samples in field testing. This is illustrated in Fig. 12.7. They also performed laboratory tests, which involved actual deposits collected from the boiler to which $ZnCl_2$ was added as 8% ZnO. The laboratory data conformed well with the field data. The temperature at which carbon steel suffered accelerated corrosion attack was found to coincide with the melting point of the boiler tube deposits. The data strongly suggest that accelerated corrosion attack in the WTE boiler combustion environment was caused by the formation of molten phases in the tube deposits.

Otsuka et al. (Ref 32) performed an extensive analysis on the salt deposits collected from three commercial WTE boilers (stoker type furnaces). A total of 23 salt deposits were collected from three boilers using corrosion probes at 550 °C (1020 °F) (probe metal temperature) for exposure of 700 and 3000 h, respectively. Each collected deposit was analyzed for the heat of fusion and the melting point by differential scanning calorimeter measurements. The heat of fusion is related to the amount of the fused salt in the deposit, with higher heat of fusion indicating a larger amount of fused salt. The deposits exhibited melting points from approximately 330 to 650 °C (625 to 1200 °F), as shown in Fig. 12.8 (Ref 32). The figure also indicates that larger amounts of salt deposits melt at around 380 and 500 °C (715 and 930 °F). In the deposits collected from the 3000 h exposure tests, sulfur (as SO_3) as high as about 40% and chlorine as high as 9%, along with Na, K, Pb, and Zn were detected. The authors observed that the corrosion attack increased with higher fused salt content in the deposits. This is illustrated in Fig. 12.9 (Ref 32) for Type 347 and alloy 625 in the corrosion probe tests. The figure shows the corrosion attack increases as the sum of the heats of fusion (or the amount of fused salt) of the deposit increases.

The salts in the deposits are mainly chlorides and sulfates. Chlorides exhibit much lower melting points than sulfates. Under the operating conditions of WTE boilers, many metal chlorides can be in a molten state in the deposits on waterwall/screen tubes (evaporator tubes) and superheaters. This is illustrated in Fig. 12.10, showing many low melting point chlorides. Approximate steam temperatures at the waterwall and superheater are shown for general comparison (Ref 30).

In Fig. 12.9, it is shown that increasing the amount of salts in the deposit could increase

Table 12.4 Corrosion rates in terms of metal loss for iron- and nickel-base alloys at 590 °C (1100 °F) for 72 h in N_2-9O_2-12CO_2-100ppmSO_2-4HCl with 0% and 10% H_2O

	Metal loss			
	0% H_2O		10% H_2O	
Alloy	µm/yr	mpy	µm/yr	mpy
Type 316	914.4	35.7	1.85	0.07
Alloy 825	20.32	0.8	3.81	0.15
Alloy 600	25.4	1.0	8.85	0.35
Alloy 625	15.75	0.6	No measurable corrosion	

1.0 µm = 0.001 mm = 0.0394 mil. Source: Ref 27

Table 12.5 Corrosion of nickel-base alloys in terms of metal loss after 500 h at 600 °C (1110 °F) in the indicated test environments

	Metal loss, µm (mils)			
Environment	C-276	600	601	214
Ar-5HCl	35 (1.4)	50 (2.0)	90 (3.5)	30 (1.2)
Ar-5HCl-10O_2	120 (4.7)	140 (5.5)	160 (6.3)	55 (2.2)

Source: Ref 28

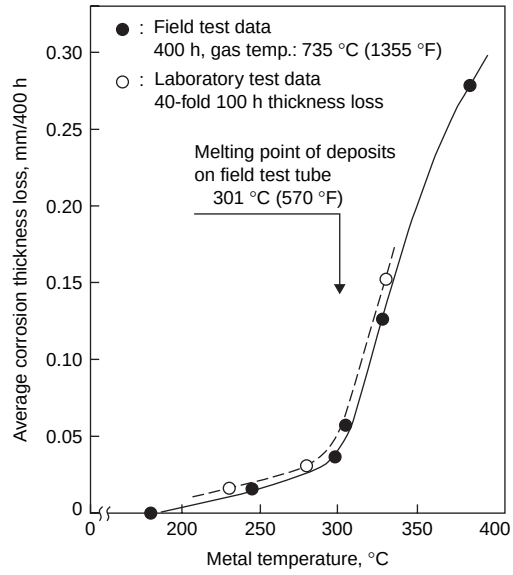

Fig. 12.7 Corrosion in terms of thickness loss for carbon steel (SA178) as a function of the metal temperature in field exposure tests. Also superimposed are data generated from laboratory tests. Source: Ref 31

the corrosion attack on the boiler tube, and Fig. 12.10 shows that there are many low-melting salts, particularly metal chlorides, that can become molten at the operating temperatures of furnace walls and superheaters. The type of chloride that forms on the deposit, as well as the type of the corrosion products formed between the chloride deposit and the underlying tube metal, can significantly affect the corrosion attack. For example, some of the eutectic chloride salts involving $FeCl_3$ can become molten at 150 to 205 °C (300 to 400 °F) as shown in Fig. 12.10. At higher metal temperatures, some chloride salts exhibit high vapor pressures. Figure 12.11 shows vapor pressures of some alkali metal salts (KCl, NaCl, KOH, and NaOH) and heavy metal chlorides ($ZnCl_2$ and $PbCl_2$) (Ref 26). K, Na, Zn, and Pb are among the most frequently detected elements in the tube deposits. It is generally believed that vapor pressures of about 10^{-4} atm are adequate to cause significant high-temperature corrosion attack. The temperature at which the vapor pressure of $ZnCl_2$ is at 10^{-4} atm is about 350 °C (660 °F) (see Chapter 6). At temperatures of 350 °C (660 °F)

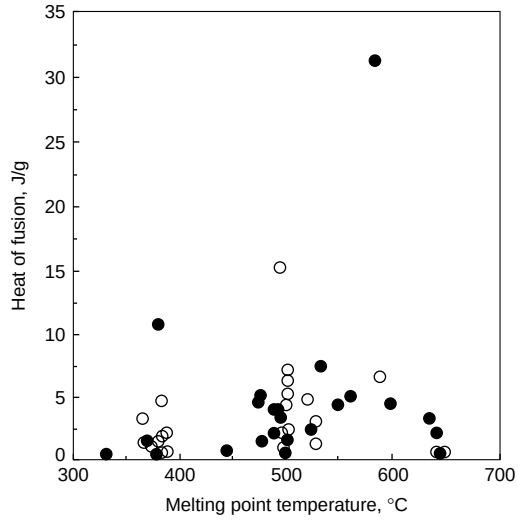

Fig. 12.8 Melting point temperatures versus the heat of fusion for the deposits collected at the corrosion probes (with the probe metal temperature of about 550 °C, or 1020 °F) in three commercial WTE boilers. The open data points are from the outer portion of the deposit, and the solid data points are from the inner portion of the deposit. Source: Ref 32

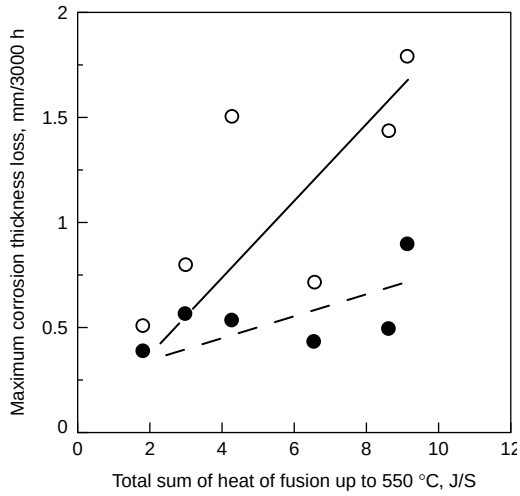

Fig. 12.9 Maximum thickness loss of corrosion probes exposed at metal temperature 550 °C (1020 °F) for 3000 h in WTE boilers as a function of the sum of heat of fusion (corresponding to the amount of fused salt) of the deposits. The open data points are Type 347H, and the solid data points are alloy 625. Source: Ref 32

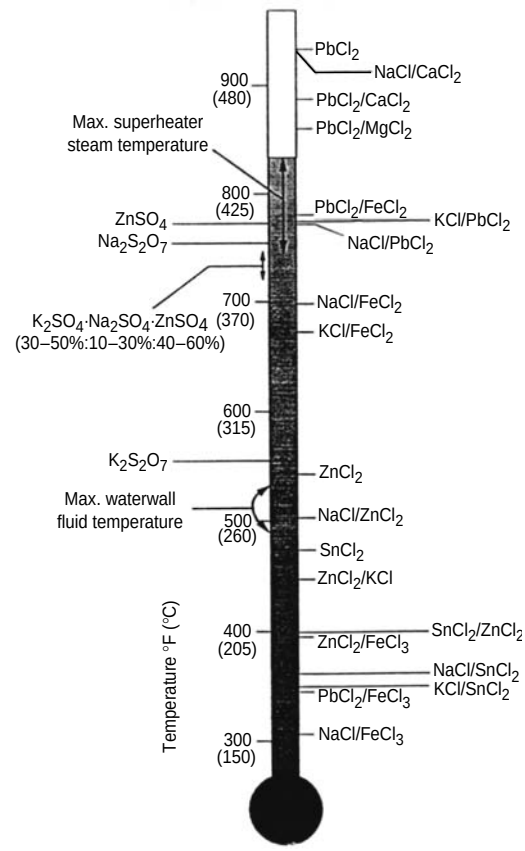

Fig. 12.10 Melting temperatures of various salts that are likely to form in WTE boilers. The temperatures of waterwall saturated fluid and superheater steam are also indicated for comparison. Source: Ref 30

and higher, vapor-phase corrosion by $ZnCl_2$ can be significant. Below this temperature, $ZnCl_2$ condenses, thus causing its vapor pressure below 10^{-4} atm and making vapor-phase corrosion less likely. Accordingly, waterwall corrosion is less likely to be caused by vapor-phase corrosion involving $ZnCl_2$. The temperature at which the vapor pressure of $PbCl_2$ is at 10^{-4} atm is about 485 °C (900 °F) (see Chapter 6). If the vapor phase of $PbCl_2$ is involved in the corrosion attack, it is likely to be for superheaters. Both KCl and NaCl will be at much higher temperatures when these chlorides reach the vapor pressure of 10^{-4} atm. Thus, both KCl and NaCl are most likely to be involved in molten salt corrosion not vapor corrosion.

Gleeson et al. (Ref 33) examined the effect of $ZnCl_2$ on the corrosion of several iron- and nickel-base alloys using a modified Dean test with a three-zone furnace arrangement. The test involved a flowing flue gas (N_2-3.6O_2-14CO_2-0.25SO_2) passing first through a crucible containing molten $ZnCl_2$ salt at 425 to 540 °C (800 to 1000 °F) to pick up $ZnCl_2$ vapor (1.3×10^{-3} atm at 425 °C, or 800 °F, and 2.8×10^{-2} at 540 °C, or 1000 °F), followed by the second zone heated to about 815 °C (1500 °F) with a catalyst to equilibrate the gas mixture, and to the third zone where specimens were exposed to a 540 °C (1000 °F) gas mixture containing $ZnCl_2$ vapor. Because the gas mixture drops in temperature from 815 °C (1500 °F) in the second zone to 540 and 510 °C (1000 and 950 °F) in the third zone where specimens were tested, the salt deposition rate onto the test specimen was found to be about 0.07 mg/cm^2 h of molten $ZnCl_2$. The test specimens were thus coated with molten $ZnCl_2$ during the testing. Their test results are summarized in Table 12.6 (Ref 33). The test temperature of 510 °C (950 °F) is very close to some superheaters with steam temperatures of about 455 to 480 °C (850 to 900 °F). The corrosion rates of alloy 625 were on the same order of magnitude as those of alloy 625 (as a weld overlay or coextruded cladding)

Table 12.6 Corrosion rates after testing for 190 h in N_2-3.6O_2-14CO_2-0.25SO_2 containing $ZnCl_2$ vapor, which condensed onto the test specimens as molten $ZnCl_2$ at a rate of 0.07 mg/cm^2 h

	Corrosion rate, mm/yr (mpy)	
Material	540 °C (1000 °F) front row	510 °C (950 °F) back row
C-2000	1.83 (72)	…
625	3.07 (121)	2.97 (117)
C-22	2.9 (114)	2.11 (83)
214	1.42 (56)	2.18 (86)
230	4.24 (167)	2.87 (113)
G-30	…	4.17 (164), 4.42 (174)
825	4.72 (186)	3.15 (124)
HR-160	2.18 (86)	3.45 (136)
HR-120	8.94 (352)	5.26 (207)
556	7.11 (280)	3.63 (143)
Type 310	7.77 (306)	…

Source: Ref 33

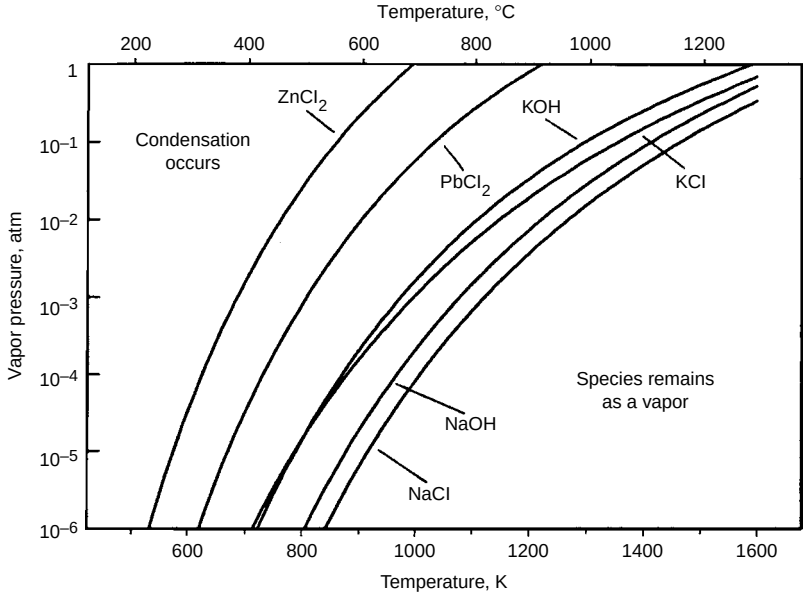

Fig. 12.11 Vapor pressures of some alkali and heavy metal salts as a function of temperatures. Source: Ref 26

in some very aggressive boilers, as shown in Fig. 12.6. It is thus believed that the severe corrosion of the alloy 625 overlay (or cladding) superheater tubes was most likely due to molten $ZnCl_2$ and/or molten $PbCl_2$. Because of considerable scattering in the data, the test results were not adequate for making an alloy ranking among nickel-base alloys. X-ray diffraction analysis of the scale and corrosion products was performed on alloys C-22, 625, G-30, 825, HR-120, and Type 310, showing mainly Cr_2O_3 and $NiCr_2O_4$ for all alloys, with $NiSO_4$ being detected for C-22, 625, 825, and Type 310 (Ref 33).

From analysis of severely corroded tube samples obtained from operating boilers, it was learned that Cl, Zn, Pb, Cd, Na, K, and S, along with major alloying elements from the tube (e.g., Fe if the tube was steel, or Cr and Ni if alloy 625 overlay) were often detected in the deposit and corrosion products. Wright et al. (Ref 16) reported that the deposits (on a severely corroded waterwall tube) were found to contain 10 to 30% chloride, 33 to 47% Pb, 3 to 13% Zn, 3 to 14% Na, and 2 to 11% K. Spiegel (Ref 12) analyzed two overlay superheater tube samples that were severely corroded in German boilers. One tube sample was overlaid with Ni-16.7Cr-8Fe-4.6Si alloy, while the other overlaid with alloy 625. In both cases, the overlays were severely corroded. Analysis of the deposits in both cases showed salt melts were sulfates in contact with the flue gas and chlorides at the deposit/scale phase boundary (Ref 12). The sulfate smelt was a $CaSO_4$-K_2SO_4-Na_2SO_4 system including $ZnSO_4$ and $PbSO_4$. The chloride melt was KCl-$ZnCl_2$ and also NaCl.

Heavy metals, such as Zn and Pb, along with Cl, have been detected in the corrosion front

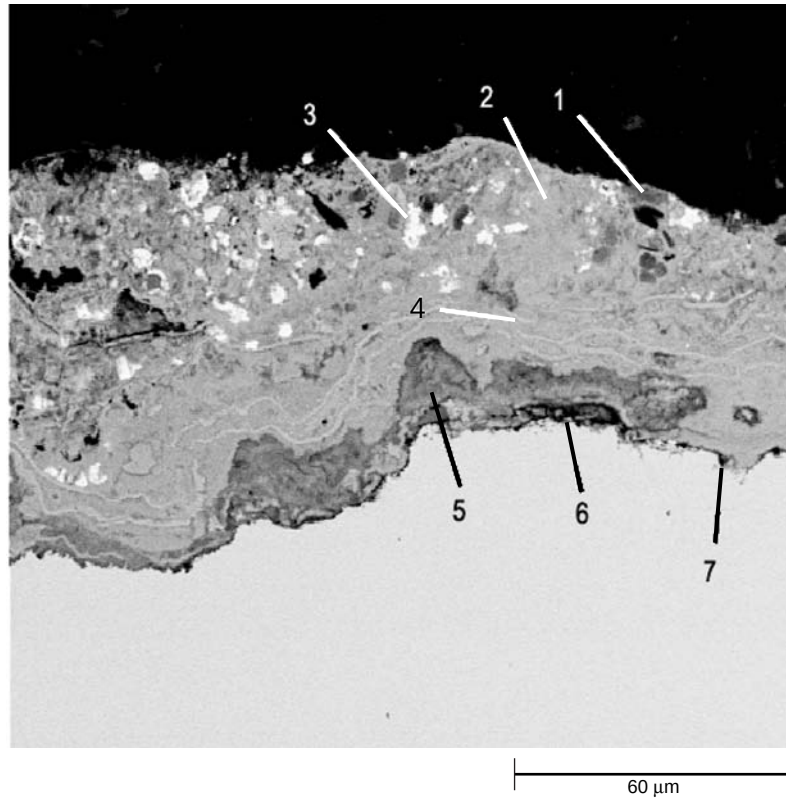

Fig. 12.12 Scanning electron micrograph (backscattered electron image) showing the deposits and corrosion scales formed on a carbon steel (SA178A) superheater tube suffering severe tube-wall wastage. Chemical compositions at different locations were analyzed by energy-dispersive x-ray spectroscopy (EDX) analysis (trace elements not reported here):
1: 31% Ca, 29% Si, 14% Mg, 15% Fe, 9% S, and 2% Zn
2: 63% Fe, 16% Cl, 9% Zn, 4% Pb, and 2% S
3: 20% Fe, 13% Cl, 3% Zn, 41% Pb, 11% S, 4% Na, 3% K, and 2% Ca
4: 67% Fe, 12% Cl, 7% Zn, 4% S, and 6% Na
5: 72% Fe, 6% Cl, 7% Zn, 4% S, 4% Na, and 2% K
6: 88% Fe, 2% Cl, 2% Zn, 2% Cd, and 1% Na
7: 76% Fe, 8% Cl, 5% Zn, 2% Cd, 2% Na, and 2% S

of superheater tubes from operating boilers (Ref 22). This is illustrated in Fig. 12.12 (Ref 22) for a carbon steel superheater tube that suffered severe corrosion attack. The steam temperature and pressure of the superheater were reported to be 400 °C (750 °F) and 4.5 MPa (625 psig), respectively. The tube wall was reportedly reduced from the original 5.6 mm (0.220 in.) to about 1.02 mm (0.040 in.) after 11 months of service, with a wastage rate of approximately 5 mm/yr (196 mpy). Figure 12.12 shows the deposit and corrosion products. The corrosion front (location No. 5, 6, and 7 in Fig. 12.12) was found to contain Cl, Zn, Cd, Na, S, and Fe. The compounds are believed to contain iron chlorides with Zn, Cd, and Na.

The composition of the deposit and corrosion products can vary significantly from plant to plant. This is shown in another boiler described in Fig. 12.13 and 12.14 (Ref 22), which involved an alloy 625 overlay superheater tube (410 °C, or 770 °F, steam) after service for about 6.5 months. Figure 12.13(a) shows the full cross section of the weld overlay with slight surface pitting attack, and Fig. 12.13(b) shows one of the corrosion pits at a higher magnification. The chemical compositions of the deposit and the corrosion products, which were analyzed by SEM/EDX, are shown in Fig. 12.14. Significant amounts of lead were found throughout the deposit and corrosion products. It is also significant that Pb, Zn, and Cl, along with Cr, Ni, and

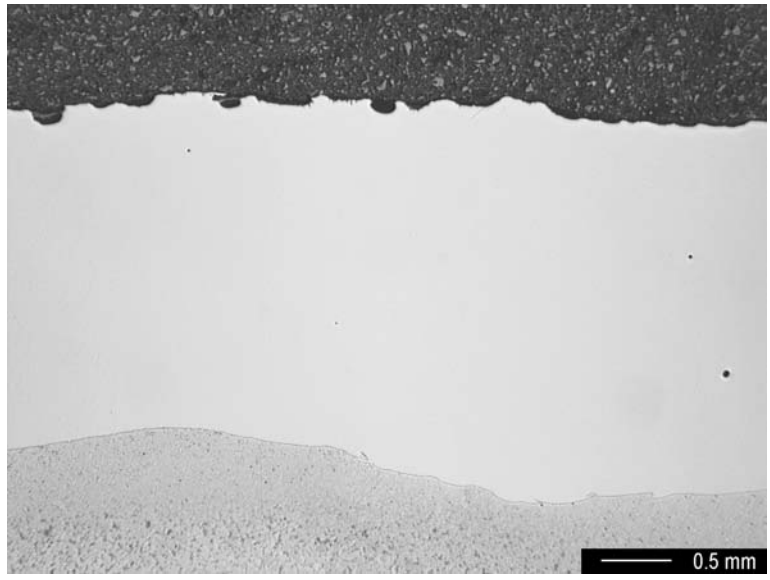

(a)

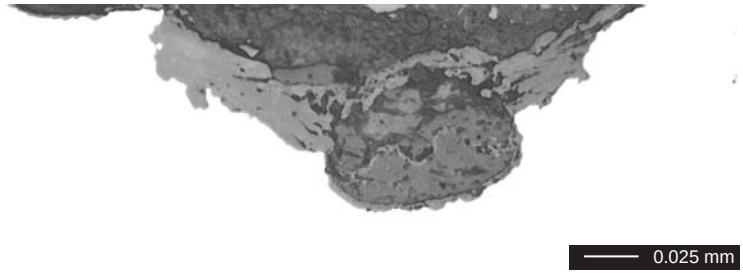

(b)

Fig. 12.13 (a) Optical micrograph showing slight pitting corrosion attack on alloy 625 overlay in an alloy 625 spiral overlay superheater tube after about 6.5 months of service. Micrograph (a) also shows the fusion boundary and substrate carbon steel. (b) Higher-magnification view of one of the corrosion pits. SEM/EDX analysis on the corrosion products in one of the surface pits is summarized in Fig. 12.14.

Mo (major alloying elements from the weld overlay) were detected in the corrosion front, as indicated in locations No. 10 and 12 in Fig. 12.14.

Both the morphology and the corrosion front that contained heavy metals, such as Zn and/or Pb, as were observed in the above two cases, suggest that the corrosion mechanism is fluxing by molten chloride salts.

In some cases, the corrosion morphology for a weld overlay of a Ni-Cr-Mo alloy involves general metal wastage followed by internal corrosion penetration along dendrites of the weld overlay. This internal dendrite corrosion attack (or penetration) is in a way similar to internal oxidation attack or intergranular oxidation attack following general oxidation (or general metal wastage by oxidation) for wrought alloys. Similarly, internal corrosion attack (or intergranular corrosion attack) also takes place in wrought alloys under gaseous chloridation attack. Figure 12.15, shows general material wastage followed by internal dendrite corrosion penetration in the overlay for an alloy 622 overlay superheater tube after 225 days of exposure. This weld overlay tube was still in excellent condition, as shown in Fig. 12.16, showing the entire cross section of this alloy 622 overlay (on

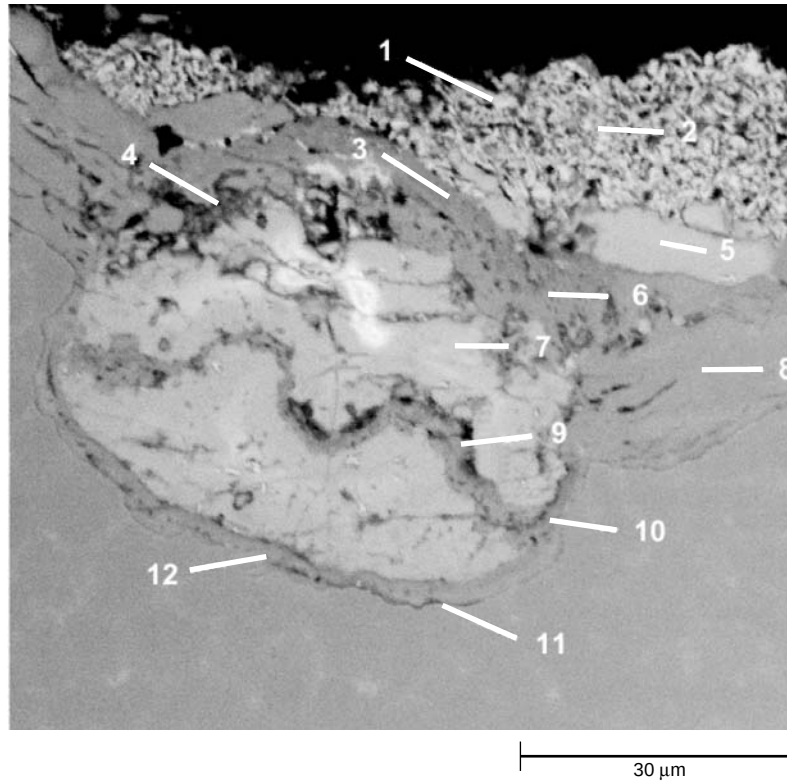

Fig. 12.14 Scanning electron micrograph (backscattered electron image) showing a localized corrosion pit on alloy 625 overlay of a superheater tube. SEM examination using energy-dispersive x-ray (EDX) spectroscopy showed the chemical compositions (wt%) at different phases, marked as No. 1 through No. 12. The chemical compositions (wt%) at different phases are:
1: 68% Pb, 11% Mo, 6% Cr, 3% Fe, 3% Ni, 4% S, 3% Cl, and trace elements
2: 63% Pb, 9% S, 6% Cl, 7% Cr, 5% Mo, 2% Fe, 3% Ni, 2% Na, and trace elements
3: 31% Cr, 24% Ni, 2% Fe, 27% Pb, 6% Zn, 5% S, 1% Cl, and trace elements
4: 32% Pb, 14% Cr, 8% Ni, 5% Fe, 10% Mo, 7% Zn, 9% Cl, 5% K, 3% Na, 3% S, and trace elements
5: 52% Pb, 11% K, 13% S, 7% Cl, 6% Mo, 4% Na, 4% Cr, 2% Ni, and trace elements
6: 34% Ni, 23% Cr, 3% Fe, 23% Pb, 7% Zn, 6% Mo, 2% Cl, and trace elements
7: 49% Pb, 12% K, 3% Na, 13% S, 7% Cl, 5% Cr, 6% Mo, 3% Ni, and trace elements
8: 30% Cr, 28% Pb, 13% Ni, 11% Zn, 7% Mo, 6% Cl, 2% K, and trace elements
9: 26% Pb, 22% Ni, 16% Cr, 11% Zn, 7% Cl, 5% Mo, 7% Na, 3% Fe, and trace elements
10: 27% Pb, 19% Cr, 14% Ni, 13% Zn, 9% Mo, 5% Cl, 4% Na, 2% K, and trace elements
11: 54% Ni, 24% Cr, 6% Pb, 5% S, 6% Fe, and trace elements
12: 27% Cr, 19% Ni, 19% Pb, 15% Zn, 9% Mo, 5% Cl, 2% K, 2% Fe, and trace elements

a carbon steel tube). The morphology of this internal dendritic corrosion penetration is believed to be the result of gaseous corrosion reactions, but not by the molten salt fluxing mechanism. In the same exposure test, an alloy 625 overlay tube was installed at the next platen on the same row as the alloy 622 overlay tube discussed in Fig. 12.15 and 12.16. After 152 days of exposure, the tube was removed for metallurgical examination. The alloy 625 overlay showed slight surface corrosion pitting attack (similar to alloy 622 overlay), but no internal dendritic corrosion attack, as illustrated in Fig. 12.17 (Ref 22). In another boiler where alloy 625 overlay superheater tube suffered severe corrosion attack, the overlay showed only general metal wastage with no internal dendritic corrosion attack (Ref 22). Montgomery and Larsen (Ref 34) also found that alloy 622 weld overlay, which was applied to the waterwall (the rear wall of the boiler in the first pass) in a WTE boiler (Haderslev plant) in Denmark, showed internal dendrite corrosion penetration after 8000 h of exposure, while alloy 625 weld overlay at a similar location tested during the same time period showed no internal dendrite corrosion penetration after 8000 h of exposure. Both overlays showed only narrow pitting corrosion attack. Nevertheless, Spiegel (Ref 12) observed similar internal dendrite corrosion attack on an alloy 625 overlay superheater tube where alloy 625 overlay suffered severe corrosion attack. He found that those internal dendrite corrosion phases were chlorides of mainly iron, chromium, and nickel, along with the corresponding oxides. He suggested that the molten chlorides reacted with oxides (formed on the metal) to produce chlorine, which then reacted with the metal to form metal chlorides.

The internal dendrite corrosion penetration is similar to internal corrosion attack within the alloy matrix or internal grain-boundary corrosion attack in wrought alloys under high-temperature gaseous corrosion, such as oxidation and chloridation. In high-temperature gaseous corrosion, the extent of internal corrosion attack can vary from alloy to alloy. Some alloys may exhibit more internal attack than others. It is important to note, however, that the alloys with less internal oxidation attack are not necessarily more corrosion resistant. There is no clear indication that the weld overlay with internal dendrite corrosion penetration would be less resistant in terms of the alloy's overall corrosion attack. It is believed that the corrosion rate due to general metal wastage by molten salt fluxing is the rate-controlling factor.

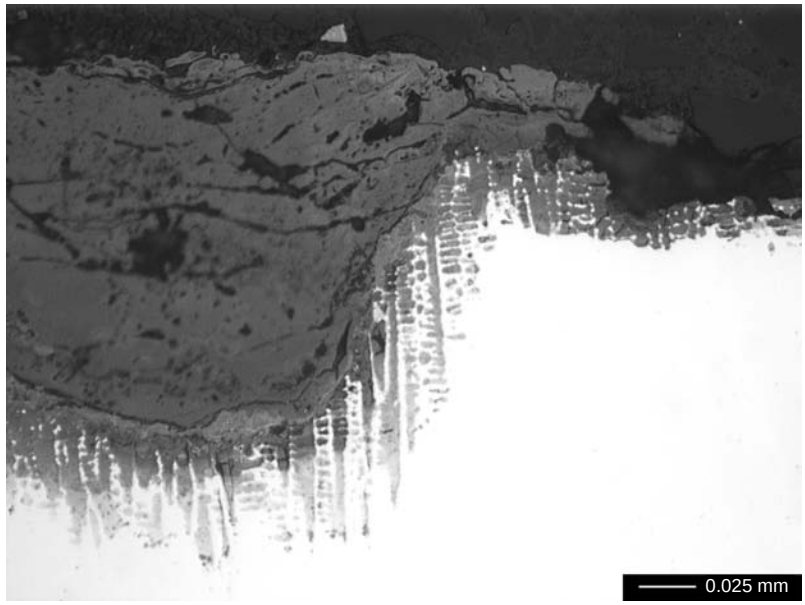

Fig. 12.15 Internal dendrite corrosion attack that followed general wastage was observed in the overlay of an alloy 622 weld overlay in an alloy 622 overlay superheater tube. Lower-magnification micrographs showing the through-thickness overlay is shown in Fig. 12.16(a) and general surface corrosion morphology is shown in Fig. 12.16(b).

12.5 Corrosion Protection for Furnace Waterwalls

In mass-burning units, the lower part of the waterwall is generally protected by refractories (e.g., SiC) (Ref 3, 7, 8, 16). The refractories provide protection for the waterwall against mechanical damage from abrasion of sliding large articles on the moving grate and also against corrosion from the combustion products. Relatively lengthy installation and upkeep time as well as reducing the heat-absorbing surface of the waterwalls can be an issue for refractory linings (Ref 20). Nevertheless, Licata et al. (Ref 17) indicated that refractory linings are needed to provide thermal insulation for ensuring that the designed combustion flue gas temperature is reached. For corrosion protection of the waterwall above the refractory, the current prevailing method is the application of alloy 625 weld overlay using automatic gas metal arc welding (GMAW) on site for existing boilers. The waterwall can also be constructed with shop-fabricated weld overlay panels with alloy 625 overlay or with coextruded composite tubes with alloy 625 cladding.

In RDF units, the same refractory design used for mass-burning units was tried initially by a major boiler designer resulting in slagging problems for the refractory wall surface (Ref 3). This was caused by the insulation of the lower furnace waterwalls by the refractory that resulted in higher flame temperatures and caused significant refractory wall slagging (Ref 3).

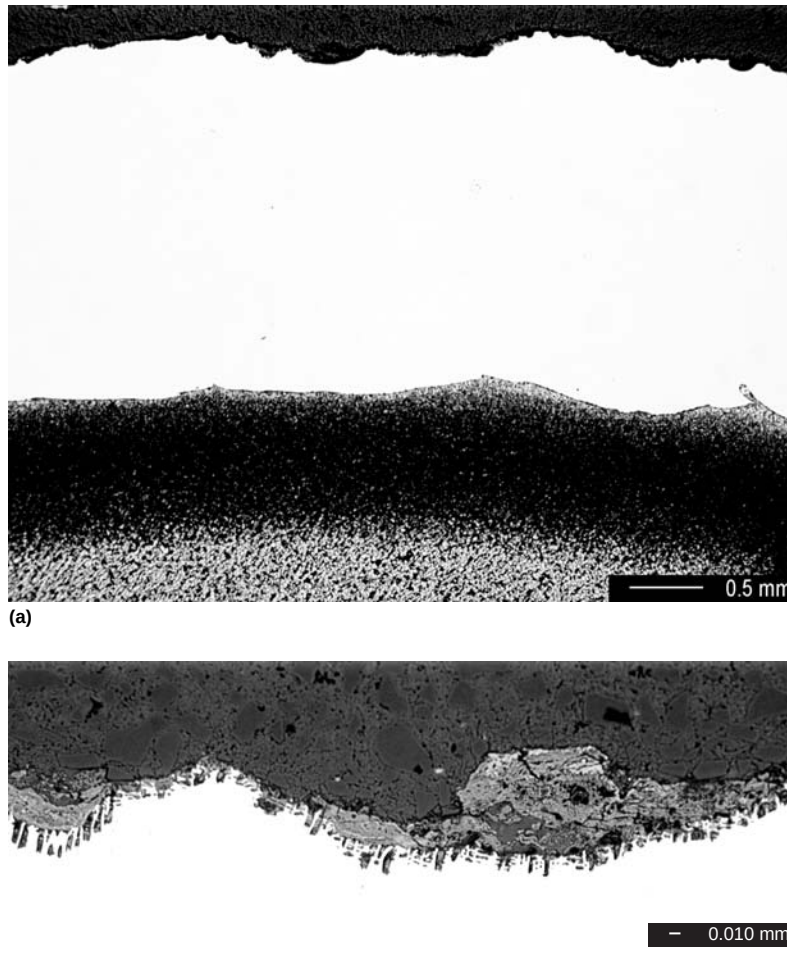

Fig. 12.16 Alloy 622 overlay superheater tube after 225 days of exposure in a boiler. (a) Cross section of the overlay showing slight pitting attack. Micrograph (a) also shows the fusion boundary and substrate carbon steel. (b) Higher-magnification micrograph showing surface corrosion morphology with general metal wastage and internal dendrite corrosion penetration

Following rapid corrosion attack of the bare carbon steel waterwalls in an RDF unit in Lawrence, MA, the lower furnace waterwall was weld overlaid with Inconel material in 1986, and this overlay protection proved to be very effective (Ref 3). The overlay alloy applied in the Lawrence unit was alloy 625 (Ref 23). The furnace waterwalls of modern RDF units are protected by alloy 625 cladding either as weld overlay applied on-site, or shop-applied panels, or as coextruded composite tubes with no refractory. Kubin (Ref 7) indicated in 1990 that the waterwalls of all Ogden RDF boilers were virtually fully covered with alloy 625 weld overlay.

Figure 12.18 shows a general view of an automatic GMAW-applied alloy 625 weld overlay on the waterwall in a boiler. Alloy 625 weld overlay on the waterwalls of the boiler was found to perform well in both mass-burning and RDF units. Generally, the wastage rates of alloy 625 overlay on waterwalls in U.S. boilers were quite low, typically approximately 125 μm/yr (5 mpy) (Ref 22, 25). The boiler tube metal temperatures are in a range of 260 to 315 °C (500 to 600 °F) for most U.S. boilers. For some European boilers running higher water/steam pressures, the waterwall tube metal temperatures could be higher.

Figure 12.19 shows the cross section of an overlaid waterwall tube sample obtained from a RDF boiler in Lawrence, MA after 16 years of service. The metallographic cross section of the alloy 625 weld overlay of that overlay waterwall tube is shown in Fig. 12.20, revealing the full

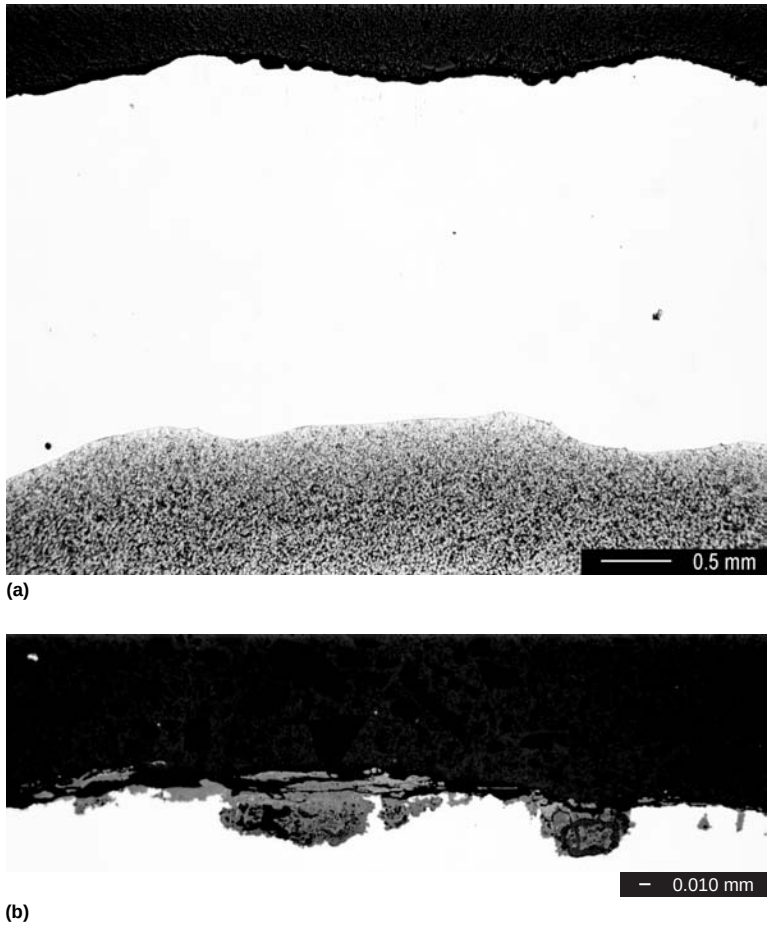

Fig. 12.17 Alloy 625 overlay superheater tube after 152 days of exposure in the superheater platen next to the alloy 622 superheater tube, which is shown in Fig. 12.16. (a) Cross section of the overlay showing slight pitting attack. Micrograph (a) also shows the fusion boundary and substrate steel. (b) Higher-magnification micrograph showing surface corrosion morphology with general metal wastage and no internal dendrite corrosion penetration.

cross section of the overlay with little evidence of corrosion attack. Figure 12.21 shows a close-up view of alloy 625 overlaid waterwall after about 10 years of service in another RDF boiler. The common mode of corrosion attack on alloy 625 weld overlay on the waterwall has been found to be pitting attack. This is illustrated in Fig. 12.22. When corrosion or pitting attack becomes extensive, the corroded waterwall area can be repaired by first grinding off the corroded metal prior to performing overlay welding, as shown in Fig. 12.23.

It has been reported by Vrchota (Ref 25) that the bare carbon steel waterwall above the weld overlaid waterwall had experienced higher wastage rates as the boiler continued to increase its service duration. As a result, the weld overlay area has been "creeping" upward gradually, leading to application of weld overlay at increasingly higher elevation in the boiler. This situation has also been experienced in other plants (Ref 22). However, there is no consensus on a technical explanation about this "phenomenon."

Thermal sprayed coatings have not yet been used on a large scale in WTE boilers. One of the major issues is related to the intrinsic characteristics of the sprayed coating in terms of interconnecting pores that allow the corrosive to permeate through the coating and cause corrosion attack at the coating/substrate interface, thus leading to spallation. Another issue is lack of automatic application system that can cover a large waterwall area in achieving a consistent quality over the large coating area. In the 1990s, some tests on sprayed coatings were performed in boilers without satisfactory results (Ref 7, 16, 35). DeVincentis et al. (Ref 35) conducted corrosion probe tests on sprayed coatings of three nickel-base alloys (Ni-Cr-Co-Si alloy HF-160,

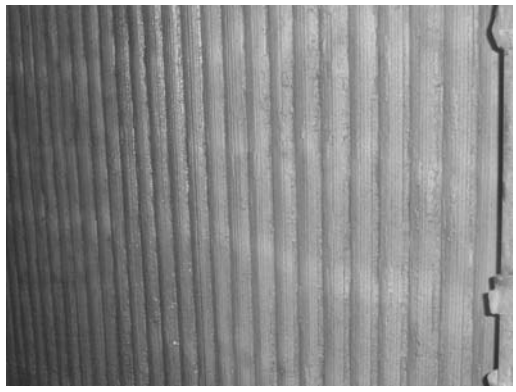

Fig. 12.18 General view of an overlaid waterwall with alloy 625 overlay in a WTE boiler. Courtesy of Welding Services Inc.

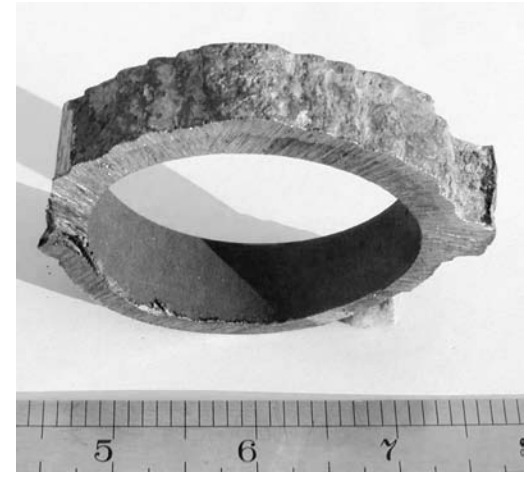

Fig. 12.19 Cross section of an overlaid waterwall tube showing alloy 625 overlay after 16 years of service in a RDF unit in Lawrence, MA. Courtesy of Welding Services Inc.

Fig. 12.20 Optical micrograph showing the cross section of the alloy 625 overlay of an overlaid waterwall sample (Fig. 12.19) obtained from a RDF boiler (Lawrence, MA) after 16 years of service. Micrograph also shows the fusion boundary and substrate carbon steel. Courtesy of Welding Services Inc.

Ni-Cr-Fe-Al-Y alloy 214, and Ni-Cr-Mo alloy C-22). The corrosion probe tests were conducted in the first pass of the front wall in a boiler at Hempstead plant for 76 days of exposure with the metal temperature maintained between 180 and 230 °C (350 and 450 °F). Coatings were applied by the inert gas electric arc spraying method. Disbonding of the coating during exposure was found to be a major problem. Alloy C-22 and 214 coatings were found to suffer disbonding after exposure. Kubin (Ref 7) indicated that a sprayed coating of alloy 50Ni-50Cr was tested in the upper furnace of a mass-burning unit and failed after 2.2 years of service. Furthermore, the removal of all the coating material in preparation for overlay welding with alloy 625 later was found to be an arduous and time-consuming operation (Ref 7).

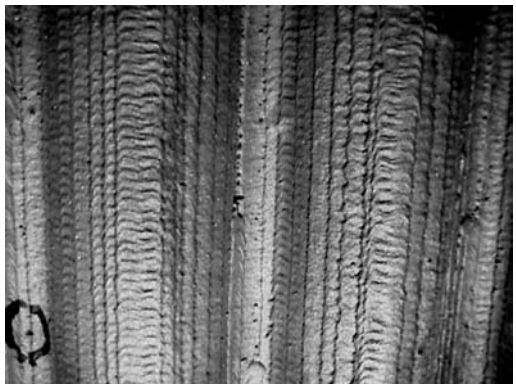

Fig. 12.21 Close-up view of alloy 625 overlay on the waterwall of another RDF boiler after 10 years of service. Shown in the photograph are two tubes and a membrane. Courtesy of Welding Services Inc.

Fig. 12.22 Pitting attack is the common mode of corrosion of alloy 625 weld overlay on the waterwall. Shown in the photograph are three tubes and three membranes.

12.6 Corrosion Protection for Superheaters

Metal temperatures for superheater tubes can be 370 to 480 °C (700 to 900 °F) or higher. In this temperature range, there will be more chloride salts that become molten, as shown in Fig. 12.10. This may also result in a higher concentration of molten chloride salts in the ash deposits forming on the tube surface. Presence of more chloride salts will result in more corrosion attack (Fig. 12.9). At higher temperatures, some of the heavy metal chlorides, such as $ZnCl_2$ and $PbCl_2$, exhibit higher vapor pressures, as shown in Fig. 12.11. This can make the environment more corrosive for superheater tube materials. As discussed in Section 12.3, premature failures of superheater tubes made of carbon or low-alloy steels were quite common. Figure 12.24 shows the cross section of a carbon steel (SA178A) superheater tube removed after 11 months of service in a mass-burning unit (Ref 22). The superheated steam temperature and pressure for this boiler were 400 °C (750 °F) and 4.5 MPa (625 psig), respectively.

Blough et al. (Ref 36) conducted corrosion probe tests in a mass-burning unit at Charleston Resource Recovery. A wide variety of commercial alloys were tested, including carbon and low-alloy steels, austenitic stainless steels, Fe-Ni-Cr alloys, and nickel-base alloys. Tests were

Fig. 12.23 Repair welding can be performed on the corroded waterwall overlay by grinding followed by overlay welding. An alloy 625 weld overlay on the waterwall after 10 years of service in a RDF unit. Shown in the photograph are two tubes and three membranes.

Fig. 12.24 Carbon steel (SA178A) superheater tube after 11 months of service in a mass-burning unit. The superheated steam temperature and pressure were 400 °C (750 °F) and 4.5 MPa (625 psig), respectively. Courtesy of Welding Services Inc.

conducted for 4492 h. The results are summarized in Fig. 12.25 (Ref 36). Alloy 625 was found to be the best at all test temperatures. Austenitic stainless steels and Fe-Ni-Cr alloys and some nickel-base alloys except alloy 625 form a big scattering band between alloy 625 and ferritic steels. In examining the wastage profiles of the probe sample cross sections, some alloys showed the maximum wastage at the 90° position, where the flue gas stream impinged upon, while others showed the maximum wastage at about 45° from either side from the 90° position. In another field test conducted in an RDF unit at Elk River Station, Blough et al. (Ref 37) reported that alloy 625 was found to perform significantly better than T-22, chromized T-22, Type 304H, HR3C, and 825 at both 470 and 500 °C (880 and 935 °F). Tests were conducted with tube samples of different alloys welded together as part of the lead superheater tubes after about 1180 h of exposure. The results are summarized in Fig. 12.26 and 12.27. The chromized layer was

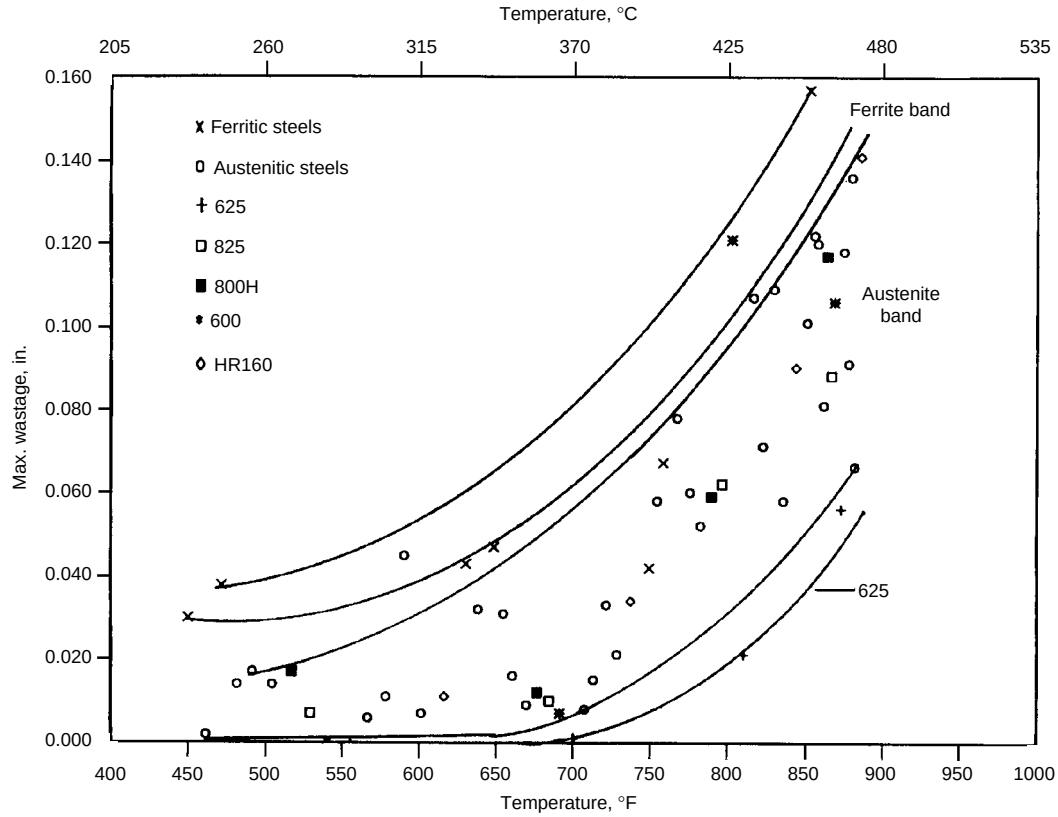

Fig. 12.25 Results of corrosion probe tests for various alloys in a boiler at Charleston Resource Recovery. The corrosion probes were installed in the convection path with the exposure time of 4492 h. Ferritic steels included carbon steel, T-22, and T-91. Austenitic steels included Type 304, 347, 310, and 27Cr-31Ni-3.5Mo (N08028). Source: Ref 36

found to be consumed in large areas and thus provided no protection. Kubin (Ref 7) had tested chromized coatings for superheater applications with mixed results, showing some success at one facility, but not at another facility. Furthermore, chromizing was not found to be cost effective (Ref 7). Other diffusion coatings, such as aluminizing and aluminum-silicon codiffusion coatings, were tested and found to be inadequate in performance (Ref 7).

Alloy 625 as a weld overlay in spiral overlay tubing or a cladding in coextruded tubing offers a viable solution to the superheater corrosion problems. Table 12.7 summarizes the comparative performance between a bare carbon steel tube and an alloy 625 overlay tube in a finishing superheater in a side-by-side field test in a boiler. The wastage rate was found to be about 2.8 mm/yr (110 mpy) for carbon steel and 0.46 mm/yr (18.3 mpy) for alloy 625 overlay. Based on these data, the expected replacement interval for carbon steel tubes and alloy 625 overlay tubes are 1.4 and 5.8 years, respectively (Table 12.7). Figure 12.5 shows alloy 625 overlay superheater tubes (405 °C, or 760 °F, and 42 bar, or 609 psi, superheated steam) exhibiting excellent overlay condition with no sign of corrosion or erosion/corrosion after 4.5 years of service in a boiler in the Netherlands (Ref 24). Alloy 625 overlay tubing has been widely used for superheater applications in WTE boilers. Alloy 625 as a cladding in coextruded composite tubes has also been widely used in WTE boilers (Ref 10).

For superheaters, the corrosiveness of the environment varies greatly from boiler to boiler. In some boilers, alloy 625 has performed well as an overlay or cladding in superheaters. One example is shown in Fig. 12.5. In some other boilers, the environment was so corrosive that alloy 625 cladding lasted for only about 1 year. For example, in boilers with superheated steam temperatures between 400 and 455 °C (750 and 850 °F), the alloy 625 cladding was found to exhibit a wide range of wastage rates from a negligible rate to 7.5 mm/yr (300 mpy), as shown in Fig. 12.6.

The factors that affect the corrosiveness of the environment can be very complex. In his corrosion probe testing in an operating boiler, Krause (Ref 29) found that the flue gas temperature could be important in affecting the corrosion rate of carbon steel. His data are shown in Fig. 12.28. The figure shows that when the flue gas

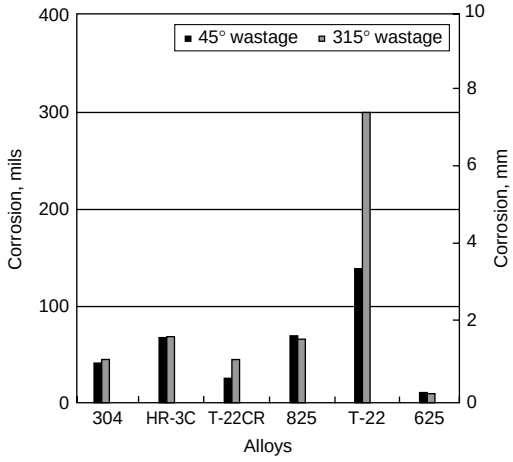

Fig. 12.26 Tube metal loss of various alloys tested at 500 °C (935 °F) for 1180 h in an RDF unit at Elk River Station. T-22CR represents the chromized T-22 tube sample. The chromized layer (on T-22) was found to be consumed in a large area. Source: Ref 37

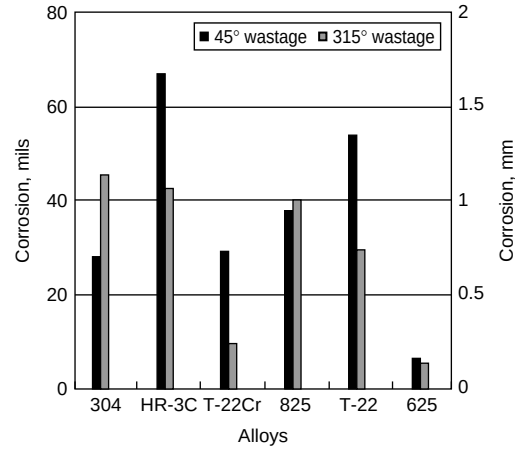

Fig. 12.27 Tube metal loss of various alloys tested at 470 °C (880 °F) for 1180 h in an RDF unit at Elk River Station. T-22CR represents the chromized T-22 tube sample. The chromized layer (on T-22) was found to be consumed in a large area. Source: Ref 37

Table 12.7 Wastage rates for the carbon steel tube and the alloy 625 overlay tube in a side-by-side test as part of a finishing superheater in a boiler in New York

	Wastage rate		
Tube construction	mm/yr	mpy	Expected tube life, years
Carbon steel	2.8	110	1.4
625 overlay	0.46	18.3	5.8(a)

(a) Overlay (0.080″ thick) + steel tube. Source: Ref 24

temperature increased from 760 to 845 °C (1400 to 1550 °F), the corrosion rate of carbon steel was found to accelerate as the metal temperature exceeded 430 °C (800 °F). The author (Ref 29) believed that the increased corrosion rate was the result of the formation of volatile $FeCl_3$, since below 430 °C (800 °F) the corrosion product was primarily $FeCl_2$, which would not volatilize at these temperatures. This flue gas temperature increase is not likely to significantly affect the corrosion rate of alloy 625, which is a nickel-base alloy and not likely to form either $FeCl_2$ or $FeCl_3$.

Metal temperature can significantly affect the corrosion rate of the alloy. The corrosion reaction is a thermally activated process, thus increasing metal temperature can result in a higher corrosion rate. Furthermore, increasing metal temperature can increase the range of various chloride salts that become molten (Fig. 12.10). Increased amounts of molten chloride salts can also increase corrosion rates. Furthermore, increasing temperature can increase vapor pressures of chloride salts, thus resulting in increased corrosion by chloride vapors.

The concentration of the chloride deposits and the type of chlorides can vary from boiler to boiler. Both the concentration of chloride salts and the type of chlorides are not normally monitored in plants. Furthermore, flue gas velocity can be an important factor in the superheater wastage. In some cases, the superheater wastage can be the result of erosion/corrosion. The only way to judge the severity of the superheater wastage issue in a particular boiler is to examine the historical data of that particular boiler. For "aggressive" boilers, efforts have been underway in the industry to identify an alloy that can outperform alloy 625. The results, however, have not been encouraging thus far. The findings of some of the comparison tests are summarized in the next paragraph.

In a side-by-side field test on alloys 625 and 622 overlay tubes (five-tube platen panel each)

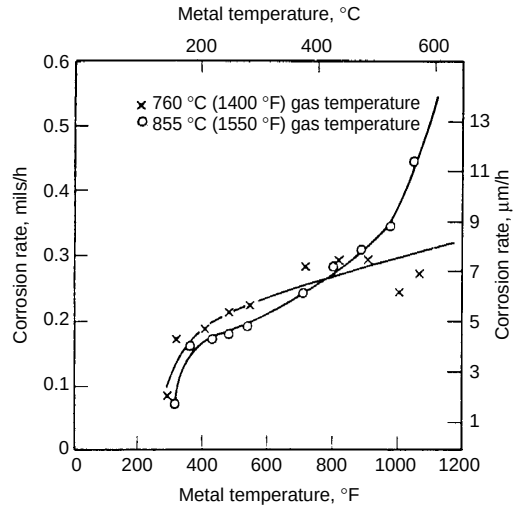

Fig. 12.28 Effect of flue gas temperature on the corrosion rate of carbon steel in short-time corrosion probe tests (10 h exposure) in an operating boiler. Source: Ref 29

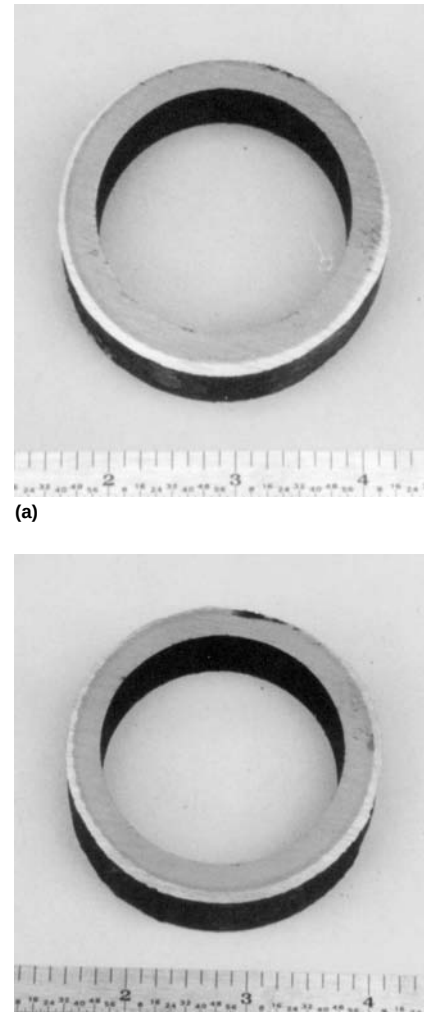

Fig. 12.29 Alloys 72 overlay superheater tube (a) and alloy C276 overlay superheater tube (b) after 7200 operating hours (10 months) in a RDF unit. The windward side of the tube, where the flue gas impinged upon the tube surface was the top side of the tube cross section as shown in the figure. The tube cross section was polished and etched with nital to reveal alloy 625 overlay (white portion of the metal) which was not etched by nital. Courtesy of Welding Services Inc.

with the steam temperature of about 340 °C (640 °F) inside the tube and about 815 °C (1500 °F) flue gas temperature, alloy 625 overlay tubes were exposed for 152 days and alloy 622 tubes for 225 days. The wastage rate was estimated to be about 175 μm/yr (7 mpy) for alloy 625 and about 355 μm/yr (14 mpy) for alloy 622. Alloy 622 containing 13% Mo and 3% W was found to be not as good as alloy 625 with about 9% Mo and no W but about 3.5% Nb. Both alloys contain about 21 to 22% Cr. Overlay tubes made of C-276 (Ni-16Cr-16Mo) and alloy 72 (Ni-44Cr) were also tested in an RDF unit, where alloy 625 overlay lasted for about 11 months. Both overlays were found to be not as good as alloy 625 overlay. The overlays of both alloys were consumed after about 10 months as shown in Fig. 12.29 (Ref 22). Alloy 686 (Ni-21Cr-16Mo-4W) was compared with alloy 625 in a side-by-side test as overlays applied to the waterwall (72 bar and 290 °C, or 555 °F) of a boiler in Denmark (Ref 34). Evaluation of the overlay waterwall samples removed from the boiler after 8000 h of exposure showed both 625 and 686 overlays exhibited shallow pitting with pitting depth of about 50 μm.

An alternate protection method for superheaters is the use of tube shields, which are typically made of Type 309, 310, and 253MA. Figure 12.30 shows carbon steel superheater tubes protected by metallic tube shields awaiting installation at a WTE plant. The shields are typically attached to the tube by mechanical straps and clamps with fillet welds. The tube shields generally do not receive adequate heat transfer through the air gap between the shield and the tube. As a result, the shields can experience temperatures as high as those of flue gas streams. The shields can thus suffer warping, distortion, and creep damage in addition to high-temperature corrosion. Accumulation of ash/salt deposits in the crevice behind the shields can further accelerate the corrosion attack. Loosened or fallen shields can cause problems by impeding the gas flow. Tube shields are generally considered to be a "sacrificial" part and are replaced regularly during the plant maintenance shutdown. Tube shields are sometimes made of cast stainless steels. A cast tube shield can be made much thicker than a wrought alloy sheet, thus enabling the tube shield to last until the next annual maintenance shutdown. Vrchota (Ref 25) reported that a 7.5 mm (0.3 in.) thick cast tube shield made of HD stainless steel (Fe-27Cr-5Ni) lasted for 12 months, which coincided with the maintenance shutdown cycle in an RDF boiler. To improve the heat transfer of the tube shield, silicon carbide cement was used to fill the gap between the shield and the superheater tube. This allows for the reinstallation of new tube shields every 12 months.

12.7 Summary

Materials issues related to waste-to-energy boilers for burning municipal solid waste (MSW) for electricity generation are presented. Combustion of MSW generates a very hostile environment for waterwall tubes and superheater tubes. The wastage rates of waterwall tubes made

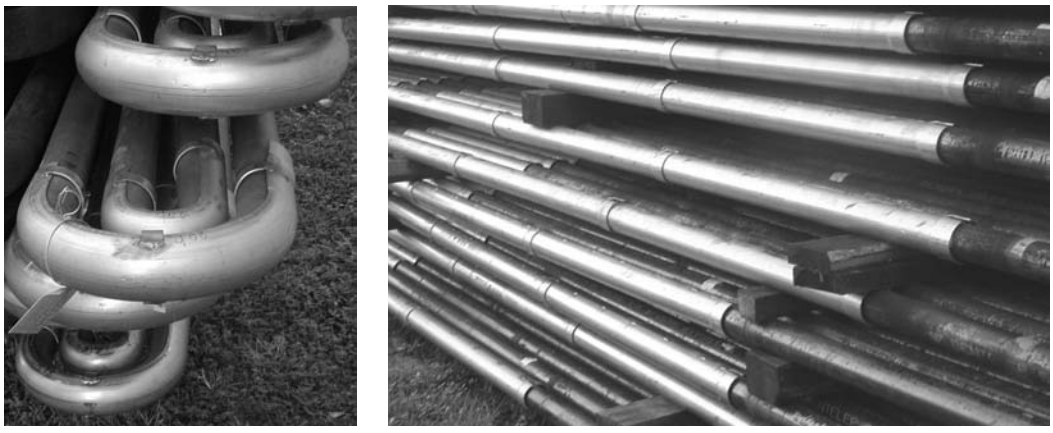

Fig. 12.30 Carbon steel superheater tubes protected by metallic tube shields awaiting installation at one WTE plant.

of carbon or low-alloy steels have been found to be unacceptably high if no protection method is used. The corrosion is believed to result from molten chloride salts. The current, widely used method for protecting the waterwalls is the use of alloy 625 overlay cladding applied by automatic gas metal arc welding process. The waterwalls can also be constructed out of alloy 625/carbon steel coextruded tubes. Superheater tubes also require some methods of protection against corrosion attack. Alloy 625 overlay tubes and coextruded tubes have been used for superheaters successfully in many boilers. However, for some boilers with higher steam temperatures and/or more corrosive environments, alloy 625 overlay or cladding was found to be inadequate. An alternate corrosion protection method is the use of metallic tube shields or refractories. Tube shields are generally considered to be a "sacrificial" part and are replaced regularly during the plant maintenance shutdown. Refractories require regular repair or replacement.

REFERENCES

1. H.H. Krause, Historical Perspective of Fireside Corrosion Problems in Refuse-Fired Boilers, Paper No. 200, *Corrosion/93,* NACE, 1993
2. G. Sorell, The Role of Chlorine in High Temperature Corrosion in Waste-To-Energy Plants, *Mater. High Temp.,* Vol 14 (No. 2/3), 1997, p 137
3. S.C. Stultz and J.B. Kitto, Ed., *Steam and Its Generation and Use,* 40th ed., Babcock & Wilcox, 1992
4. C.F. Knights, I.W. Cavell, and B.A. Phillips, Corrosion During Incineration of a Sulfur and Chlorine Bearing Mixture of Rubbers and Plastics, *Werkst. Korros.,* Vol 40, 1989, p 163
5. E.A. Bretz, Energy from Wastes, *Power,* March 1990, p S-1
6. P. Rademakers, W. Hesseling, L.A. Tange, and R. Montaigne, "Review on Corrosion in Waste Incinerators, and Possible Effect of Bromine," CEF-12, Laan van Westenenk, The Netherlands, 2002
7. P.Z. Kubin, Materials Performance and Corrosion Control in Modern Waste-To-Energy Boilers Applications and Experience, Paper No. 90, *Corrosion/99,* NACE International, 1999
8. L. Strach and D.T. Wasyluk, Experience with Silicon-Carbide Tiles in Mass-Fired Refuse Boilers, Paper No. 219, *Corrosion/93,* NACE, 1993
9. R.L. Anderson, Wheelabrator Technologies Inc., private communication, 2006
10. A. Wilson, U. Forsberg, M. Lundberg, and L. Nylof, Composite Tubes in Waste Incineration Boilers, *Stainless Steel World 99 Conference on Corrosion-Resistant Alloys* (Conf. Proc.), Book 2, KCl Publishing BV, The Netherlands, 1999, p 669
11. F. Soutrel, C. Rapin, P. Steinmetz, and G. Pierotti, Corrosion of Fe, Ni, Cr and Their Alloys in Simulated Municipal Waste Incineration Conditions, Paper No. 428, *Corrosion/98,* NACE International, 1998
12. M. Spiegel, Salt Melt Induced Corrosion of Metallic Materials in Waste Incineration Plants, *Mater. Corros.,* Vol 50, 1999, p 373
13. M. Noguchi et al., Experience of Superheater Tubes in Municipal Waste Incineration Plant, *Mater. Corros.,* Vol 51, 2000, p 774
14. P.L. Daniel, L.D. Paul, and J. Barna, Fire-Side Corrosion in Refuse-Fired Boilers, *Mater. Perform.,* May 1988, p 20
15. J.G. Singer, Ed., *Combustion Fossil Power,* 4th ed., Combustion Engineering, Inc., Windsor, CT, 1991
16. I.G. Wright, H.H. Krause, and R.B. Dooley, A Review of Materials Problems and Solutions in U.S. Waste-Fired Steam Boilers, Paper No. 562, *Corrosion/95,* NACE International, 1995
17. A.J. Licata, L.A. Terracciano, R.W. Herbert, and U. Kaiser, Design Features for Superheater Corrosion Control in Municipal Waste Combustors, *Materials Performance in Waste Incineration Systems,* G.Y. Lai and G. Sorell, Ed., NACE, 1992, p 5-1
18. H.H. Krause and I.G. Wright, Boiler Tube Failures in Municipal Waste-To-Energy Plants: Case Histories, Paper No. 561, *Corrosion/95,* 1995
19. A. Pourbaix, Corrosion of a Waste Incinerator: Effects of Design and Operating Conditions, *Werkst. Korros.,* Vol 40, 1989, p 157
20. A.L. Plumley, W.R. Roczniak, and E.C. Lewis, Materials Performance of Heat Transfer Surfaces in A MSW-Fired Incinerator, *Materials Performance in Waste Incineration Systems,* G.Y. Lai and G. Sorell, Ed., NACE, 1992, p 7-1
21. W.G. Schuetzenduebel, I.E. Johnson, and C.W. Clemons, Accelerated Tube Metal

Wastage in Municipal Solid Waste Fired Furnaces, *Materials Performance in Waste Incineration Systems,* G.Y. Lai and G. Sorell, Ed., NACE, 1992, p 10-1
22. Welding Services Inc., unpublished data, Norcross, Georgia
23. P.N. Hulsizer, Problems and Solutions in Applying Weld Overlay to Waste Boiler Incinerators, *Materials Performance in Waste Incineration Systems,* G.Y. Lai and G. Sorell, Ed., NACE, 1992, p 11-1
24. G.Y. Lai, "Corrosion Mechanisms and Alloy Performance in Waste-To-Energy Boiler Combustion Environments," presented at the 12th North American Waste To Energy Conference (NAWTEC 12) (Savannah, GA), May 17–19, 2004
25. S. Vrchota, Fireside Corrosion Management in RDF Waste-To-Energy Boilers, Paper No. 5317, *Corrosion/2005,* NACE International, 2005
26. L.D. Paul and P.L. Daniel, Corrosion Mechanisms in Oxidizing, Reducing, and Alternating Combustion Gases in Refuse-Fired Boiler Environments, Paper No. 216, *Corrosion/93,* NACE, 1993
27. G.D. Smith and P. Ganesan, Metallic Corrosion in Waste Incineration: A Look at Selected Environmental and Alloy Fundamentals, *Heat-Resistant Materials II* (Conf. Proc.), Second International Conference on Heat-Resistant Materials, K. Natesan, P. Ganesan, and G. Lai, Ed., ASM International, 1995, p 631
28. F. Devisme, P. Falgoux, F. Lefebvre, and T. Flament, "High Temperature Corrosion in Atmospheres Containing Hydrogen Chloride," presented at the 11th International Incineration Conference (Albuquerque, NM), May 11–15, 1992
29. H.H. Krause, Chlorine Corrosion in Waste Incineration, *Materials Performance in Waste Incineration Systems,* G.Y. Lai and G. Sorell, Ed., NACE, 1992, p 1–1
30. I.G. Wright, V. Nagarajan, and H.H. Krause, Paper No. 201, *Corrosion/93,* NACE, 1993
31. Y. Kawahara and M. Kira, Corrosion Prevention of Waterwall Tube by Field Metal Spraying in Municipal Waste Incineration Plants, *Corrosion,* Vol 53 (No. 3), 1997, p 241
32. N. Otsuka, Y. Tsukaue, K. Nakagawa, Y. Kawahara, and K. Yukawa, A Corrosion Mechanism for the Fireside Wastage of Superheater Materials in Waste Incinerators, Paper No. 157, *Corrosion/97,* NACE International, 1997
33. B. Gleeson, J.E. Barnes, and M.A. Harper, Corrosion Behavior of Various Commercial Alloys in a Simulated Combustion Environment Containing ZnCl2, Paper No. 196, *Corrosion/98,* NACE International, 1998
34. M. Montgomery and O.H. Larsen, Field Investigation of Various Weld Overlays in a Waste Incineration Plant, Paper No. 5309, *Corrosion/2005,* NACE International, 2005
35. D.M. DeVincentis, S.P. Goff, J.W. Slusser, Z. Zurecki, and J.T. Rooney, Solving Fireside Corrosion in MSW Incinerators with Thermal Spray Coatings, Paper No. 198, *Corrosion/93,* 1993
36. J.L. Blough, G.J. Stanko, and M.T. Krawchuk, In Situ Materials Testing in a Waste-To-Energy Power Plant, *Mater. High Temp.,* Vol 14 (No. 2/3), 1997, p 181
37. J.L. Blough, G.J. Stanko, W.T. Bakker, and T. Steinbeck, Superheater Corrosion in a Boiler Fired with Refuse-Derived Fuel, *Heat-Resistant Materials II* (Conf. Proc.), Second International Conference on Heat-Resistant Materials, K. Natesan, P. Ganesan, and G. Lai, Ed., ASM International, 1995, p 645